Article:
Burluka, AA, Gaughan, RG, Griffiths, JF et al. (3 more authors) (2016) Turbulent burning rates of gasoline components, Part 2-Effect of carbon number. Fuel, 167. pp. 357-365. ISSN 0016-2361

https://doi.org/10.1016/j.fuel.2015.11.068

Published in Fuel, Volume 167, March 2016, pp. 357-365

Turbulent Burning Rates of Gasoline Components, Part 2 - Effect of Carbon Number

A.A. Burluka[a], R.G. Gaughan[b], J.F. Griffiths[c], C. Mandilas[a,*], C.G.W. Sheppard[a], R. Woolley[d]

[a] School of Mechanical Engineering, The University of Leeds, Leeds LS2 9JT, UK

[b] ExxonMobil Research and Engineering Company, Paulsboro Technical Center, 600 Billingsport Road, Paulsboro, NJ 08066, United States

[c] School of Chemistry, University of Leeds, Leeds, LS2 9JT, United Kingdom

[d] The University of Sheffield, Department of Mechanical Engineering, Mappin Street, S1 3JD, UK

[*] Corresponding author. Present address: The Centre for Research and Technology, Hellas, Chemical Process & Energy Resources Institute, 3km Charilaou-Thermi Road, Thermi 57001, Greece

mandilas@cperi.certh.gr

Abstract

Experimental measurements of turbulent and laminar burning velocities have been made for premixed hydrocarbon-air flames of straight chain molecules of increasing carbon number (from n-pentane to n-octane). Measurements were performed at 0.5 MPa, 360 K and rms turbulent velocities of 2 and 6 m/s, for a range of equivalence ratios. The laminar burning velocities were used to interpret the turbulent data, but were also found to be broadly in line with those of previous workers. At lean conditions the turbulent burning velocity was measured to be similar between the four alkanes studied. However, at rich conditions there were notable differences between the turbulent burn rates of the fuels. The equivalence ratio of the mixtures at which the maximum burning velocities occurred in the turbulent flames was richer than that under laminar conditions. The equivalence ratio of the peak turbulent burning velocity was found to be a function of the carbon number of the fuel and the turbulent intensity and became gradually fuel rich with increases in each of these values.

Keywords: laminar flames, turbulent flames, burning velocity, hydrocarbon combustion

1. Introduction

This is the second part of a two paper series presenting the measurement of turbulent burning velocities for hydrocarbons of different molecular structure under conditions typical of those seen in industrial applications. The main aim of the current work was to investigate the effects of fuel molecular structure and equivalence ratio, ϕ, on the laminar and turbulent burning velocity of growing premixed flames (deflagrations) and allow for direct comparison. The turbulent burning velocity is a function of those physico-chemical features of a fuel-air mixture encapsulated in its laminar burning velocity, u_l, and the turbulence characteristics of the flow field within the engine. The influence of fuel structure on the laminar burning

velocity has been reported [e.g. 1-5]. However, experimental studies on the influence of hydrocarbon molecular structure on burn rate under turbulent conditions typical of those seen in industrial applications are sparse [6-7].

Presented in this paper are experimentally determined laminar and turbulent burn rates for a set of straight chain hydrocarbons of varied carbon number, n-pentane, n-hexane, n-heptane and n-octane. These fuels are representative components of automotive gasoline blends. Measurements of their laminar burning velocity have been performed by a number of previous workers at a range of conditions [2, 4, 8-9]. Apart from the size of the carbon chain, which affects the number of breakdown steps needed during oxidation, another significant difference anticipated to have impact on burn rate, is the differing molar mass of the fuels selected for this study and, thus, their differing Lewis Number (or Markstein Number). This is expected to be especially important under turbulent conditions, as there is plenty of experimental evidence demonstrating the significance of fuel diffusion in premixed turbulent flames.

2. Experimental

Only brief details of the experiments are given here, further information can be found in Part 1 of this two part study [10]. Also described in [10] are the well-established methods on which laminar and turbulent burn rate calculations were based. The Leeds MkII spherical bomb operating under laminar and turbulent conditions, was employed for the studies. The effects on burn rate of two different turbulent rms velocities were examined (u' = 2 m/s and 6 m/s). All experiments employed schlieren-based imaging. Laminar flames were recorded at 2000 frames/s. Turbulent flames were photographed at rates of 6300 and 9000 frames/s, for u' = 2 and 6 m/s, respectively. All deflagrations were initiated with a spark at a nominal initial temperature of T_i = 360 K and pressure of P_i = 0.5 MPa and were conducted for a range of

equivalence ratios, from lean ($\phi \sim 0.8$) to rich ($\phi \sim 1.6$). The burning velocity was determined during the so-called “pre-pressure” period, during which the pressure rise caused by compression from the propagating flame was much smaller than the initial pressure; in the case of the vessel used the pressure rise at the full radius of the windows (75 mm) was less than 3%.

At least two laminar and five turbulent deflagrations were performed at each condition. For laminar flames, the repeatability tolerance was set at a maximum of 2% in the time elapsed from ignition required to reach a pressure of 0.75 MPa for tests conducted on the same day; and 3% for tests conducted on different days. Turbulent tests exhibited inherent shot-to-shot variability and thus a similar tolerance approach could not be followed; typical experimental scatter for turbulent flames was circa 10% (in terms of coefficient of variance, COV, of burn rate), independent of the rms turbulent velocity.

3. Results and Discussion

3.1 Laminar flame propagation and cellular flames

As all the measurements in this study were performed at elevated initial pressure of 0.5 MPa, the majority of flames became ‘cellular’ shortly after ignition. The term ‘cellularity’ is used to describe the result of both hydrodynamic and thermo-diffusive instabilities observed in laminar flames where the flame surface develops irregular patterns, or ‘cells’, of varying dimensions. This phenomenon is known to accelerate the burn rate, by increasing the surface area of the flame and by modifying the composition of the flame front. The development of cellular structure in expanding spherical flames has been linked to the ratio of thermal to mass diffusivity, i.e. the Lewis number, *Le*, of the deficient reactant [11-13]. Values of Lewis numbers for the fuels examined here were determined at Ti = 360 K and Pi = 0.5 MPa, via $Le = \alpha_{mix} / D_{\text{deficient reactant}}$, where α_{mix} is the thermal diffusivity of the mixture and $D_{\text{deficient reactant}}$ is the

mass diffusivity of the deficient reactant. Determination of the transport properties followed the approach described in [14]. The results are displayed in Table 1. All lean mixtures examined were calculated to have $Le > 1$, with the lighter n-pentane exhibiting the lower *Le* and the heavier n-octane, the higher *Le*. The *Le* values of the rich mixtures explored were computed to be from 0.9 to 0.95.

For $Le < 1$, flames are intrinsically unstable [11]. For the apparatus used and conditions explored in this study cellularity occurred very early in flame development; typically 10-15 mm in mean flame radius. For $Le > 1$, the cellularity onset has been predicted to occur when the flame reaches a certain critical radius, r_{crit} [11]. Predictions based on this theory are not valid at near stoichiometric conditions, where $Le \approx 1$ [12]. There may be other factors, such as heat loss, hydrodynamic stretch or gravity, which also affect the development of the cellular structure [13].

Identifying the onset of cellularity from experimental data can be ambiguous. For schlieren measurements, r_{crit}, has been defined as the point where small scale cells appear on the flame surface [11]. It is implicit, due to the progressively growing nature of these cracks, that definition of r_{crit} by photographic observations is subject to discrimination by the human eye and the quality of the optics employed. An alternative way of defining r_{crit} is by relating it to the point at which an appreciable flame acceleration (a_f) appears on the plot of stretched burning velocity (u_n) vs. mean flame radius [15, 16]. In the typical burn rate data of Figure 1, a noticeable a_f is observed at a radius of ca. 25 mm.

For the vast majority of flames examined here, the difference between the visual determination of r_{crit} and that determined graphically [16] was within 1.5 ms (~3 frames), or 2-3 mm in mean flame radius. The values of r_{crit} displayed in Figure 2 are based on combined graphical and photographic evidence (i.e. cross verification of one method against the other), with error margins estimated at ±2 mm in radius.

For the alkanes investigated, r_{crit} decreased with ϕ and no major differences between the fuels were found at a given equivalence ratio. It has been described [11, 15], that the propensity of a flame to become cellular is closely linked to the value of L_b. This correlates to the results of Figure 3, where values of burned gas Markstein length, L_b, are plotted against r_{crit} (Figure 3); an almost linear increase in r_{crit} with L_b was found for all fuels studied. A similar increase of r_{crit} with Markstein number, (Ma), given by the ratio of L_b over the laminar flame thickness (δ_l), has previously been reported in [17].

Of interest with respect to the effects of cellularity on flame propagation are the flame acceleration results, a_f, derived from stretched burning velocities, u_n, and shown in Figure 4. Note that these results do not include n-hexane, as tests for this fuel were performed in slightly different equivalence ratios compared to the rest of the alkanes. For the lean case (ϕ = 0.8) all flames remained smooth within the visible radius defined by the vessel's windows, as the thermo-diffusive effects, coupled with stretch, stabilise flames with $Le > 1$ [11, 12]. As a consequence, no acceleration due to cellularity was observed.

Typically for all fuels examined, for ϕ = 1.1 following the spark affected region (i.e. for mean flame radius > 8 mm) flame acceleration was small and approximately constant up to around mean flame radii above 20 mm. At r_u > 20mm, acceleration increased, becoming significantly more marked at radii of 25 mm, which correspond to the typical r_{crit} values of the fuels at this equivalence ratio. Thereafter, flames continued to accelerate sharply, reaching peak acceleration at ~40 mm mean flame radii. Subsequently, flame acceleration fell, reaching low pre-cellularity rates by mean flame radii of circa 50 mm.

The flames for ϕ = 1.2 followed a similar pattern to that noticed for ϕ = 1.1, although with earlier development of cellularity (occurring soon after the spark affected region), the initial low and constant acceleration 'plateau' are less obvious and the peak accelerations and return

to low pre-cellularity levels occur sooner. A similar pattern can also be observed at ϕ =1.4, with even earlier cellularity development within the spark affected region.

The occurrence of significant flame acceleration at the critical flame radius for the onset of cellularity is caused by an associated increase in flame surface area [18]. An alternative, or possibly additional, reason for the increase in flame acceleration at the onset of cellularity arises from considerations of linear flame stability analysis based on high activation energy asymptotics [12]. The kinematics of a curved flame front dictate that, if the burning velocity is the same along the front, the trailing parts of a cell consume the fresh gas faster than the leading parts, per unit frontal area. A simple heuristic model predicted that flame acceleration will reduce to zero, when an equilibrium is attained between the leading and the trailing parts [19]. However, while the results shown in Figure 4 seem to support this model qualitatively, the theory assumes that flame perturbations (i.e. the depth of cells) are small compared to flame size, which is limited strictly to the initial acceleration period. In addition, numerical comparison is complicated by the effects of stretch rate, flame growth and short observation period.

To clarify the trend in a_f, cell size development was examined in schlieren images taken around the middle of the vessel window. To quantify the average cell size, magnified grayscale flame images were further processed in MATLAB, first by converting them into black & white format and then by counting the number of pixels in each of the “white islands” corresponding to the flame cells, subsequently to obtain a mean cell flame area in mm^2. These average cell area results are displayed in Figure 5, for ϕ = 1.1 and 1.4. In general, average cell areas rapidly decreased after the onset of cellularity. For ϕ = 1.1, minimum cell areas generally occurred at flame radii of 10-15 mm after those at the onset of cellularity. For ϕ = 1.4, cells achieved their minimum size slightly faster (5-10 mm in mean flame radius after r_{rit}). Fully-developed cell areas for ϕ = 1.4 flames were 80% (for n-heptane and

n-octane) smaller than those for the ϕ = 1.1 flames. With respect to the relative behaviour between the different fuels, the lighter and more diffusive fuel, n-pentane, had the largest average fully-developed cell area, followed by n-heptane and n-octane. These results suggest a correlation between cell-size and flame acceleration. The point at which cell sizes attained their minimum values coincided well with that in reaching peak acceleration, see Figure 4 cf. Figure 5. Similar correlation also existed between average cell areas and peak accelerations. This is consistent with flame acceleration resulting from the transition from a smooth surfaced flame into a fully cellular flame and its associated increase in flame surface area. Once a constant fully developed cell size is reached, the increase in flame surface area per unit volume of the flame ceases and flame acceleration returns to the pre-cellular values.

3.1 Laminar Burning Velocity

The measured u_l results for all fuels studied are shown in Figure 6, plotted against ϕ. Solid lines correspond to 3rd order polynomial fits in the unstretched burning velocity data determined via the techniques described in [10, 17]. Dashed lines correspond to 3rd order polynomial fits for u_l values computed using $u_l = u_{n,\min}$ (i.e. equivalent to $L_b = 0$), where, $u_{n,min}$ is the minimum stretched entrainment burning velocity measured. All rich flames for the alkanes examined showed signs of cellularity as early as a mean flame radius of 10-15 mm. Consequently, too few data points were available to determine L_b. Burning velocities obtained in this way cannot be considered to be rigorously defined but represent a pragmatic approach to obtaining laminar burning velocity data to aid the analysis of subsequent turbulent burning measurements. Also included in the plot are indicative error bars. The uncertainty of lean to mildly rich flames was estimated at circa 2%, typical of that for u_l obtained via the methods described in [10, 17]. In an effort to quantify the maximum possible impact of setting u_l equal to $u_{n,min}$, the error bars for $\phi > 1.1$ also incorporated extrapolation of measured L_b values to

equivalence ratios of up to ϕ = 1.6. By doing so, the maximum possible error in laminar burning velocity at the extreme rich conditions explored in the study was estimated at approximately 7%.

All fuels studied were found to have their maximum u_l at $\phi \sim 1.1$. There was hardly any variation in u_l between lean fuel-air flames, as is also evident in the flame speed measurements by Davis and Law [2] for 1 bar and 300 K counter-flow measurements and Farrell *et. al*. [4] for spherical flames in a bomb. Increased laminar burn rate differences were apparent at fuel rich conditions with n-pentane typically being the slowest fuel and n-octane the fastest fuel. However, as mentioned above, the laminar burn rate data for $\phi > 1.1$ are not strictly defined u_l, hence possible cellularity effects might be encapsulated in these data.

The Markstein length of a flame is a physico-chemical flame parameter, customarily used to characterise the effect of stretch rate on flame speed [15]. High positive values of L_b indicate that as the flame expands, and becomes increasingly less stretched, there is a gain in flame speed; the opposite is true for flames with negative L_b values. For reasons already explained, Markstein lengths could not be experimentally determined for $\phi > 1.1$, hence measurements shown in Figure 7 refer to fuel-air mixtures of up to ϕ = 1.1. Positive values of L_b were measured for all fuels up to $\phi \leq 1.1$. Differences were within experimental scatter, nonetheless, the lightest n-pentane was measured to have consistently lower Markstein lengths, while the heaviest n-octane had consistently the higher L_b.

Laminar burn rates measured in this study were compared to laminar burn rate data for alkane-air flames, reported by Law *et. al*. [5, 8] and measured in a combustion vessel at 0.5 MPa and 353 K (Figure 8). The agreement between the measurements of the two studies was overall good, albeit current measurements were consistently higher compared to

corresponding u_l values in [5, 8]. Maximum differences of up to 10% between the two studies were found for lean (ϕ = 0.8) n-pentane and rich (ϕ = 1.1) n-octane.

The experimentally determined values of u_l were also compared to u_l calculated via the Premix code in CHEMKIN [20, 21], at the same unburned temperature and pressure of 360 K and 0.5 MPa. Multi-component formulation for transport properties including Soret diffusion were used. The JetSurF 2.0 [22] mechanism was selected as it was possible to compare the fuels considered with a single mechanism. The comparison was performed for n-pentane through n-heptane and is included in plots (a) to (c) of Figure 8. There was good agreement between the experiments and model at lean ϕ. For ϕ > 1.1, the flames were cellular shortly following ignition so the experimental data corresponds to the minimum burning velocity recorded. It is to be expected that cellularity increases the burn rate [11, 18], so this might explain why the measured values were higher than the computed values. Nonetheless, such comparison is only qualitative as the flames do not exist as a single uninterrupted flame front under these conditions, because thermo diffusive effects would result in localized quenching of the flame surface [15]. However, the computed u_l could provide a useful, unambiguously defined reference although they cannot be experimentally realised.

The development of hydrocarbon kinetic mechanisms, allied with improvements in u_l experimental methods, has resulted in better understanding of the key combustion processes taking place within the flame [4-5, 23-26]. Unimolecular decomposition of the primary fuel can readily occur at the temperatures that prevail in the reaction zone of a premixed flame, promoted by kinetic energy transfer during collisions between molecules. The weakest bonds within the primary fuel, the saturated C-C linkages, are the most susceptible to fragmentation. However, there is another possibility for decomposition of the longer chain n-alkanes (e.g. at C > 5) due to the flexibility of the molecular chain. In this process intramolecular energy transfer may occur as a result of one end of the chain colliding with a site at or close to the

other end [27]. This is illustrated in Figure 9 as an interaction between a primary and a secondary bound H atom, and the inference is that excess energy would accumulate in one or other of the C-H bonds. The secondary C-H bond would be the more susceptible of the two to decomposition, by virtue of its lower bond strength, but the main significance is that fragmentation must yield an alkyl radical and an H atom, rather than the two alkyl radicals, predominantly produced in the more general intermolecular collisional process. As in unimolecular reactions, the rate at which the decomposition can occur is limited by the vibrational frequency of the bond to be broken and a statistical (or steric) factor which relates to the probability of the intramolecular interaction taking place. This route for H atom generation can only contribute to the burn rates measured for the longer chain n-alkanes (n-hexane, n-heptane and n-octane) under fuel rich conditions; this is thus a potential mechanism contributing to the observed higher burning rate of heavier hydrocarbons.

3.2 Turbulent Burning Velocity

The techniques used for determination of the turbulent burn rates are described in [10]. Sample results of measured turbulent burning velocities, u_{te}, plotted against mean flame radius for n-octane flames are displayed in Figure 10. Note that the subscript ‘e’ in u_{te} denotes that this definition is based on entrainment of unburned gas [29]. Contrary to the observations for laminar rich flames, where there was transient and large acceleration for a short period following the onset of cellularity, turbulent rich flames continuously accelerated throughout flame development within the vicinity of the bomb windows.

The experimental scatter in the measured turbulent burning velocity, u_{te}, was ~10% COV for all turbulent flames studied and proved independent of u'. This was in accord with previous measurements in this vessel [28]. Displayed in Figure 11 are measured u_{te} values for the n-alkane dataset, under turbulent rms velocities of u' = 2 and 6 m/s, plotted versus ϕ. Note

that the u_{te} values refer to the burn rate at a mean flame radius of 30 mm; reasons behind selecting this mean flame radius for presentation of the results are discussed in [10]. Also included in the plot of Figure 11 are the laminar burning velocities to allow for direct comparison. The curves are 3rd order polynomial fits to the measured data, added for better illustration.

The peak u_{te} values obtained were similar for all alkane fuels tested. On the basis of the maxima of the 3rd order fits, for u' = 2 m/s the maximum u_{te} was ~ 1.7 m/s, with n-pentane statistically having the lowest $u_{te,max}$ value, at 1.66 m/s, and n-octane the highest, at 1.72 m/s. Likewise, for u' = 6 m/s the average peak burn rate was measured to be ~ 3.7 m/s, with n-hexane having the lowest peak burn rate, at 3.64 m/s, and n-heptane the highest, at 3.78 m/s. In comparison, peak laminar burn rates ranged between 0.37 m/s (n-pentane) to 0.39 m/s (n-octane). Overall, the increase in the maximum u_{te} attained by increasing u' from 2 to 6 m/s accorded to $u_{te,max} \sim (u')^{0.73}$, which is similar to that described by Zimont in his turbulent flame closure combustion model [30].

The maximum turbulent burning velocities, connected via dashed lines in Figure 11, were attained for rich mixtures and, more importantly, the equivalence ratios at which they were observed increased with turbulence and fuel molecule size. This is a qualitative difference between turbulent and laminar flames, as the laminar flames generally burned fastest at $\phi \sim$ 1.1 for all fuels. The degree of burn rate enhancement due to turbulence, expressed as u_{te} / u_l, is shown in Figure 12 and can be clearly seen to vary with ϕ; for all fuels there was a distinctive increase in u_{te} / u_l for fuel rich conditions, particularly so for $\phi \geq$ 1.2. The displacement of the maximum burning rate towards rich mixtures reported here, was firstly observed as early as 1955 [31]; however, this observation received little attention until relatively recently [32].

As for the laminar flames, differences between the values of u_{te} for fuel lean turbulent conditions were found to be very small for all fuels and increased at fuel rich conditions. The trend in ranking of turbulent burn rate resembled that with respect to ranking in u_l. The lightest alkane tested, n-pentane, was measured to burn noticeably slower at extreme rich turbulent conditions of $\phi \geq 1.4$ in comparison to its larger alkane counterparts. Normal hexane also appeared to burn slightly slower to its larger alkane counterparts, particularly so under milder turbulence. However, this finding was less conclusive, as the differences in turbulent burn rate between n-hexane, n-heptane and n-octane were generally within experimental scatter. Based on the above, it could be argued that fuel effects were not found to be significant for conditions where fuel was the deficient reactant.

There have been studies comparing turbulent flames with the same laminar burning velocity but differing thermo-diffusive properties, some of which are summarized in [33]. It was demonstrated that flames with lower Lewis numbers (or Markstein numbers) burn faster under turbulent conditions. This was also reflected here, as the u_{te} / u_l results shown in Figure 12 revealed higher gains under turbulence for rich conditions, where L_b shown in Figure 7 and *Le* based on deficient reactant, see Table 1, were lower for all fuels. Experimental measurements of turbulent flames with low Markstein numbers have identified changes in the structure of the flame front, associated with the local curvature [34], as have DNS studies [35-37]. Where the flame front is convex to the unburned reactants, high radical concentrations are observed, with localized quenching occurring where the flame is concave.

Whilst some effort has been made to incorporate the effects described above into turbulent burning velocity expressions and theories, notably by Bradley *et al*. [38], the laminar flame part is often solely represented by u_l and thus thermo-diffusive effects are neglected. An older concept that is presently being reconsidered is that of critically curved “leading points” of the flame front; i.e. those parts of the flame most advanced into the fresh gas lead the

propagation. As these leading points are convex to the unburned mixture it has been suggested that they are subject to thermo-diffusive enhancement resulting in locally leaner (and faster) flames. Subsequently, Borghi *et. al*. [39], made the alternative suggestion that the leading points are critically curved rather than strained. Recently, Venkateswaran *et. al*. [40] were able to correlate the turbulent consumption speed using the maximum stretched laminar burn rate, but could not collapse data for differing pressures. The leading edge hypotheses predicts that for heavier hydrocarbons the maximum turbulent burning rates should be exhibited by rich flames; however, the ϕ at which the maximum is attained should not depend on the turbulence level, which was observed here.

Despite recent advances in detailed computations there remains a demand for simpler expressions to predict the turbulent burning velocity, based on easily obtained parameters, although whether this is feasible is debatable. A study with iso-octane demonstrated that a selection of the existing expressions were unable to capture the trend of u_t with ϕ [41]. A number of workers have attempted approximate quantification of the influence of Markstein number on burn rate for turbulent premixed combustion [42-43]. Displayed in Figure 13 are average experimental u_{te} / u_l values, generated in the current study, plotted against L_b. A consistent trend was observed, with the ratio of u_{te} / u_l decreasing with L_b for each of the two rms turbulent velocities; similar effects were described in [28, 32]. Results such as this may well form the basis of future empirical turbulent burning velocity expressions.

4. Conclusions

In his review of premixed turbulent combustion, Driscoll [44] asked the question ‘‘how important are thermodiffusive effects for fully turbulent conditions?’’. Using available experimental and numerical studies he found evidence that thermodiffusive effects are significant even in highly turbulent flames; this is confirmed with these experiments. In the

majority of experimental studies examining this phenomenon, flames of identical laminar burning velocity but differing Markstein (or Lewis) numbers have been compared. Whilst the above approach is useful at demonstrating this phenomenon, this study demonstrates that fuel, equivalence ratio and turbulence levels are all of significance. The complexity of the combustion of premixed turbulent flames is increased, as more wide ranging modelling studies and extensive experimental databases are presented. However, there remains the requirement for relatively simple expressions to predict the turbulent burning velocity within models of industrial applications and the results presented here may point towards future developments in this area.

The most important conclusions of the study are highlighted below.

- The laminar burning velocity of n-pentane, n-hexane, n-heptane and n-octane were found to be almost identical for equivalence ratios varying from ca. 0.8 to 1.1. All fuels examined were measured to have their peak u_l values at $\phi \sim 1.1$. Under rich conditions u_l could not be measured as the spherically laminar flames were observed to be cellular from ignition. In these cases u_l was estimated using the minimum observed flame speed, $u_{n,min}$. Values of $u_{n,min}$ increased with the molecular weight of the fuel, here relating to the number of carbons in its molecule.
- Under laminar conditions at 0.5 MPa, cellularity enhances the burn rate. However, findings from the current study suggest that, for the rig used in this study and the fuels and conditions explored, cellularity-induced flame acceleration lasts for typically 15-20 mm following the cellularity onset, before returning back to values similar to those observed during the pre-cellular phase. Thermodynamic flame instabilities noted under laminar conditions did not appear to have any effects under corresponding turbulent conditions.

- Although the magnitude of peak turbulent burning velocity was measured to be similar for all fuels at both turbulent rms velocities studied, peak u_{te} values did not occur at the same ϕ as the $u_{l.}$ The peak burning velocity shifted to increasing ϕ under turbulent conditions. The magnitude of the shift increased with length of carbon chain and turbulence intensity. For instance, for n-pentane, the laminar burning velocity peaked at $\phi \sim 1.1$, while u_{te} at $u' = 6$ m/s was maximum at $\phi \sim 1.3$. In the case of the heavier n-octane at $u' = 6$ m/s, the peak turbulent burning velocity occurred at $\phi \sim 1.5$, i.e. much richer compared to the peak in u_l at $\phi \sim 1.1$.
- At lean ϕ, the turbulent burning velocity was observed to be similar for the four fuels studied. However, at rich fuel conditions, there were notable differences between the turbulent burn rates of the alkanes examined. The above observation was thoroughly replicated under laminar conditions.

Acknowledgements

The support of Mercedes-Benz High Performance Engines is gratefully acknowledged.

References

[1] Gerstein, M., Levine, O., Wong, E.L., **Flame Propagation. II. The Determination of Fundamental Burning Velocities of Hydrocarbons by a Revised Tube Method**, J Am Chem Soc 73 (1951) 418

[2] Davis, S.G., Law, C.K., **Determination of and Fuel Structure Effects on Laminar Flame Speeds of C1 to C8 Hydrocarbons**, Combust Sci Technol 140 (1998) 427

[3] Vagelopoulos, C.M., Egolfopoulos, F.N., **Direct Experimental Determination of Laminar Flame Speeds**, P Combust Inst 27 (1998) 513

[4] Farrell, J.T., Johnston, R.J., Androulakis, I.P., **Molecular Structure Effects On Laminar Burning Velocities At Elevated Temperature And Pressure**, SAE Tech Paper (2004) 2004-01-2936

[5] Wu, F., Kelley, A.P., Law, C.K., **Laminar flame speeds of cyclohexane and mono-alkylated cyclohexanes at elevated pressure**, Combust Flame 159 (2012) 1417

[6] Burluka, A.A., Gaughan, R.G., Griffiths, J.F., Mandilas, C., Sheppard, C.G.W., Woolley, R., **Effects of Hydrocarbon Fuel Structure on Experimental Laminar & Turbulent Burn Rates**, 7th European Combustion Meeting, Budapest, 2015

[7] Wu, F., Saha, A., Chaudhuri, S., Law, C.K., **Propagation speeds of expanding turbulent flames of C4 to C8 n-alkanes at elevated pressures: Experimental determination, fuel similarity, and stretch-affected local extinction**, Proc Combust Inst, 35 (2015), 1501

[8] Kelley, A.P., Smallbone, A.J., Zhu, D.L., Law, C.K., **Laminar flame speeds of C5 to C8 n-alkanes at elevated pressures: Experimental determination, fuel similarity, and stretch sensitivity**, P Combust Inst 33 (2011) 963–970

[9] Ji, C., Dames, E., Wang, Y.L., Wang, H., Egolfopoulos, F.N., **Propagation and Extinction of Premixed C5-C12 n-Alkane Flames**, Combust Flame, 157 (2010), 277

[10] Burluka, A.A., Gaughan, R.G., Griffiths, J.F., Mandilas, C., Sheppard, C.G.W., Woolley, R., **Turbulent Burning Rates of Gasoline Components, Part 1 - Effect of Fuel Structure of C6 Hydrocarbons**, Fuel, xxx (2015), xxx, in press

[11] Bradley, D., Harper, C.M., **The development of instabilities in laminar explosion flames**, Combust Flame 99 (1994) 562

[12] Bechtold, J.K., Matalon, M., **The dependence of the Markstein length on stoichiometry**, Combust Flame 127 (2001) 1906

[13] Law, C.K., **Dynamics of stretched flames**, Symp (Inter) Comb 22 (1989) 1381

[14] Bird, R.B., Stewart, W.E., Lightfoot, E.N., **Transport Phenomena, Revised 2nd Edition,** John Wiley & Sons, 2007, ISBN 0470115394

[15] Bradley, D., Sheppard, C.G.W., Woolley, R., Greenhalgh, D.A., Lockett, R.D., **The development and structure of flame instabilities and cellularity at low Markstein numbers in explosions**, Combust Flame 122 (2000) 195

[16] Mandilas, C., "**Laminar and turbulent burning characteristics of hydrocarbon fuels**", PhD Thesis, University of Leeds, 2008

[17] Bradley, D., Hicks, R.A., Lawes, M., Sheppard, C.G.W., Woolley, R., **The measurement of laminar burning velocities & markstein numbers for i-octane–air and i-octane–n-heptane–air mixtures at elevated T and P in an explosion bomb**, Combust Flame 115 (1998) 126

[18] Wu F., Jomaas G., Law C.K., **An experimental investigation on self-acceleration of cellular spherical flames**, Proc Comb Inst 34 (2013) 937

[19] Zeldovich Y.B., Barenblatt G.I., Librovich V.B., Makhviladze G.M., **Mathematical Theory of Combustion and Explosion**, Plenum Publ. Corp., N.Y.,1985

[20] Kee, R.J., Grcar, J.F., Smooke, M.D., Miller, J.A., **A FORTRAN Program for Modeling Steady Laminar One-dimensional Premixed Flames**, Sandia Report, SAND85, 8240, Sandia National Laboratories, 1985

[21] Grcar, J.F., Kee, R.J., Smooke, M.D., Miller, J.A., **A Hybrid Newton/Time-Integration Procedure for the Solution of Steady, Laminar, One-Dimensional, Premixed Flames**, 21st Symp (Int) Comb (1986) 1773

[22] Wang, H., Dames, E., Sirjean, B., Sheen, D.A., Tango, R., Violi, A., Lai, J.Y.W., Egolfopoulos, F.N., Davidson, D.F., Hanson, R.K., Bowman, C.T., Law, C.K., Tsang, W., Cernansky, N.P., Miller, D.L., Lindstedt, R.P, **A high-temperature chemical kinetic model of n-alkane (up to n-dodecane), cyclohexane, and methyl-, ethyl-, n-propyl and n-butyl-cyclohexane oxidation at high temperatures**, JetSurF version 2.0, September 19, 2010

[23] Egolfopoulos, F.N., Zhu, D.L., Law, C.K., **Laminar flame speeds at 1 atm in C2H6-air mixtures**, Symp (Inter) Comb 23 (1991) 471

[24] Hu, E., Huang, Z., He, J., Miao, H., **Experimental and numerical study on laminar burning velocities and flame instabilities of hydrogen–air mixtures at elevated pressures and temperatures**, Int J Hydrogen Energ 34 (2009) 8741

[25] Dryer, F.L., Westbrook, C.K., **Chemical kinetic modeling of hydrocarbon combustion**, Prog Energ Combust 10 (1984) 1

[26] Johnston, R.J., Farrell, J.T**., Laminar burning velocities and Markstein lengths of aromatics at elevated temperature and pressure**, P Combust Inst 30 (2005) 217

[27] Gaughan, R., **Private Communication**, 2007

[28] Ormsby, M.P., **Turbulent Flame Development in a High-Pressure Combustion Vessel**, University of Leeds, 2005, Thesis

[29] Gillespie, L., Lawes, M., Sheppard, C.G.W., Woolley, R., **Aspects of Laminar and Turbulent Burning Velocity Relevant to SI Engines**, SAE Tech Paper (2000) 2000-01-0192

[30] Zimont, V.L., **Gas premixed combustion at high turbulence, turbulent flame closure combustion model**, Exp Therm Fluid Sci 21 (2000) 179

[31] Wohl, K., Shore, L., **Burning velocity if unconfined turbulent flames. Experiments with butane-air and methane-air flames**, Ind Eng Chem 47 (1955) 828

[32] Lawes, M., Ormsby, M.P., Sheppard, C.G.W., Woolley, R., ., **Variation of turbulent burning rate of methane, methanol, and iso-octane air mixtures with equivalence ratio at elevated pressure**, Combust Sci Technol 177 (2005) 1273

[33] Lipatnikov A.N., Chomiak J., **Lewis Number Effects in Premixed Turbulent Combustion and Highly Perturbed Laminar Flames**, Combust Sci Technol 137 (1998) 277

[34] Haq, M.Z., Sheppard, C.G.W., Woolley, R., Greenhalgh, D.A. and Lockett, R.D., **Wrinkling and curvature of laminar and turbulent premixed flames**, Combust Flame 131 (2002) 1

[35] Bell, J.B., Cheng, R.K., Day, M.S., Shepherd, I.G., **Numerical simulation of Lewis number effects on lean premixed turbulent flames**, Proc Comb Inst 31 (2007) 1309

[36] Aspden, A.J., Day, M.S., Bell, J.B., **Characterization of Low Lewis Number Flames**, Proc Comb Inst 33 (2011) 1463

[37] Day, M.S., Gao, X., Bell, J.B., **Properties of Lean Turbulent Methane-Air Flames with Significant Hydrogen Addition**, Proc Comb Inst 33 (2011) 1601

[38] Bradley, D., Lau, A.K.C., and Lawes, M., **Flame stretch rate as a determinant of turbulent burning velocity**, Phil Trans R Soc 338 (1992) 359

[39] Borghi, R., **Turbulent combustion modelling**, Prog Energ Combust 14 (1988) 245

[40] Venkateswaran, P., Marshall, A., Seitzman, J., Lieuwen, T., **Pressure and fuel effects on turbulent consumption speeds of H2/CO blends**, Proc Comb Inst 34 (2013) 1527

[41] Lawes, M., Ormsby, M.P., Sheppard, C.G.W., Woolley R., **The turbulent burning velocity of iso-octane/air mixtures**, Combust Flame, 159 (2012) 1949

[42] Bray, K.N., Peters, N., **Turbulent Reactive Flows – Laminar Flamelets in Turbulent Flows**, Academic Press, 1994

[43] Weiß, M., Zarzalis, N., Suntz, R., **Experimental study of Markstein number effects on laminar flamelet velocity in turbulent premixed flames**, Combust Flame 154 (2008) 671S

[44] Driscoll, J.F., **Turbulent premixed combustion: Flamelet structure and its effect on turbulent burning velocities**, Prog Energ Combust Sci 34 (2008) 91

Table 1 – Lewis numbers for the alkane-air mixtures at the equivalence ratio range explored in the current study, computed at 360 K and 0.5 MPa using the techniques described in [14].

ϕ	n-pentane	n-hexane	n-heptane	n-octane
0.8	2.30	2.58	2.84	3.10
0.9	2.28	2.54	2.81	3.06
0.99	2.25	2.51	2.77	3.02
1.01	0.96	0.95	0.95	0.95
1.1	0.95	0.95	0.94	0.94
1.2	0.95	0.94	0.93	0.93
1.4	0.93	0.93	0.92	0.92
1.6	0.92	0.91	0.91	0.90

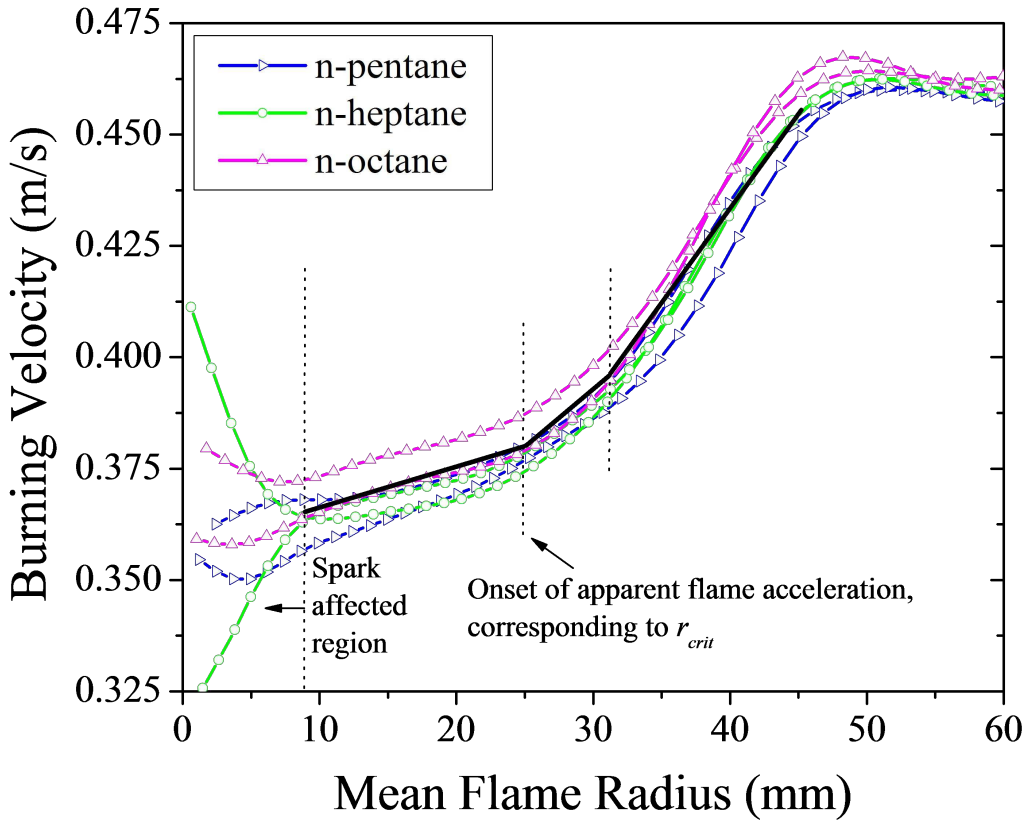

Figure 1 – Cellularity induced acceleration showing its graphically defined onset. Results displayed are for sample ϕ = 1.1 flames.

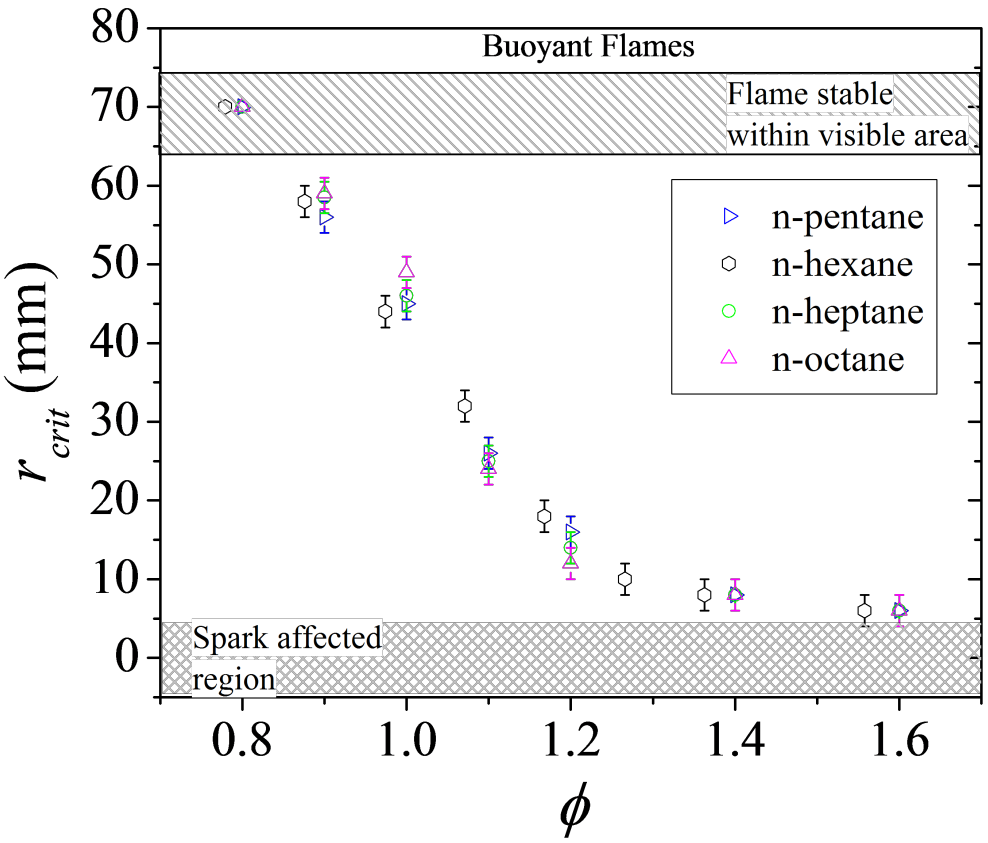

Figure 2 – Critical flame radii derived from photographic and graphical observations. Error bars of ± 2 mm are displayed.

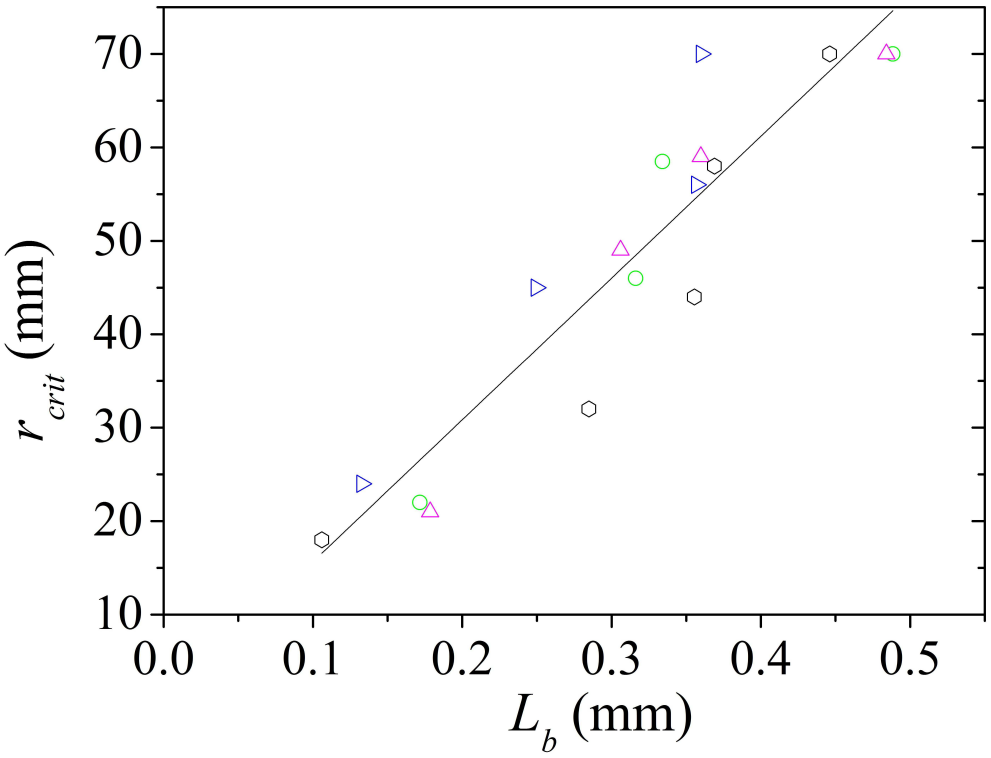

Figure 3 – Correlation between r_{crit} and L_b.

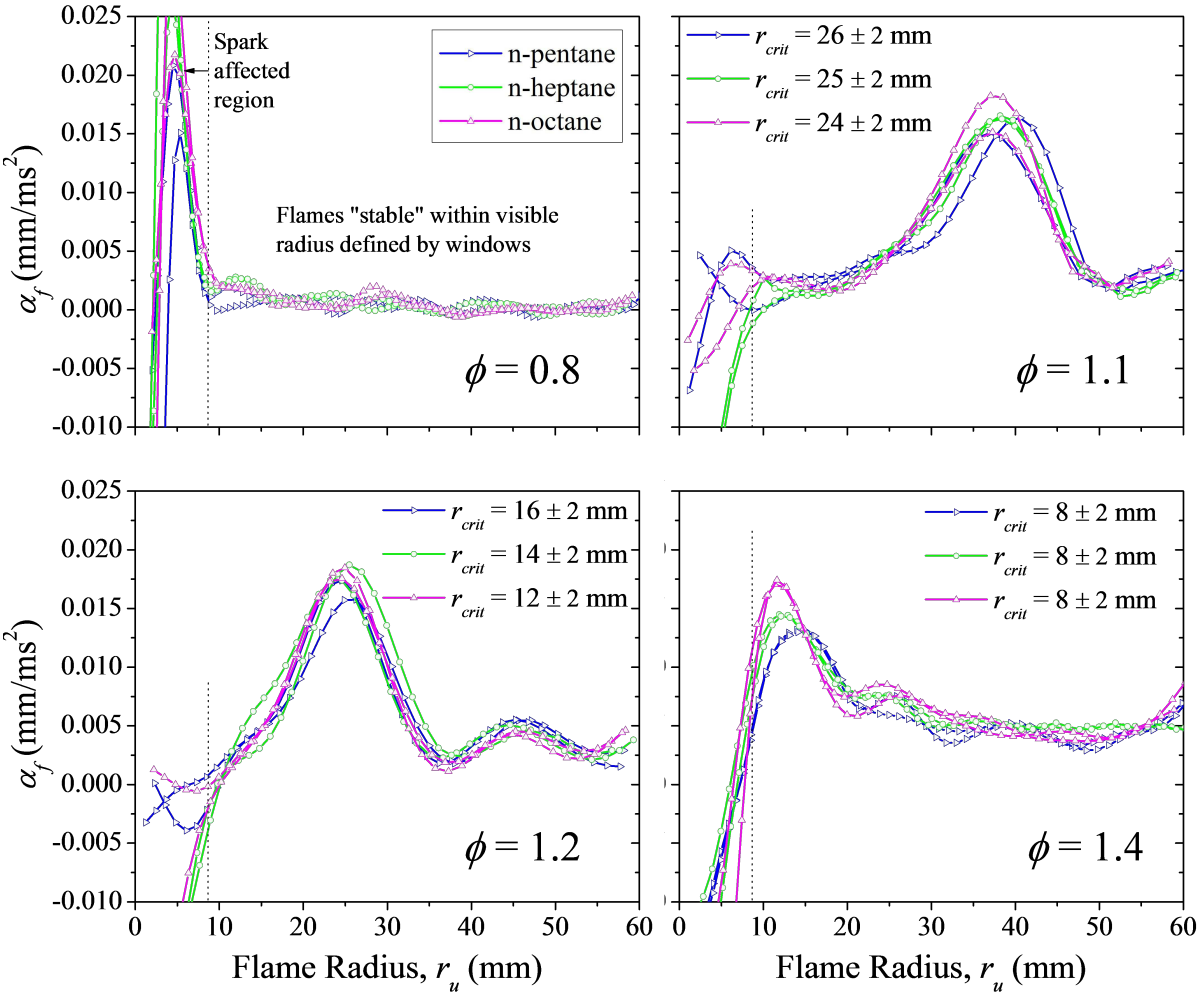

Figure 4 – Flame acceleration, $a_f = du_n / dt$, for different ϕ, highlighting the effects of cellularity on flame propagation.

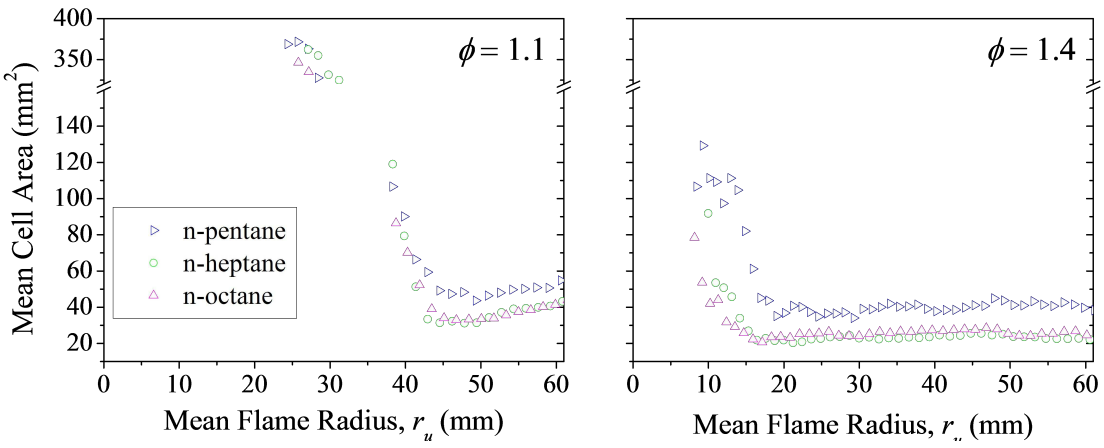

Figure 5 – Mean cell areas as determined from schlieren images of cellular flames.

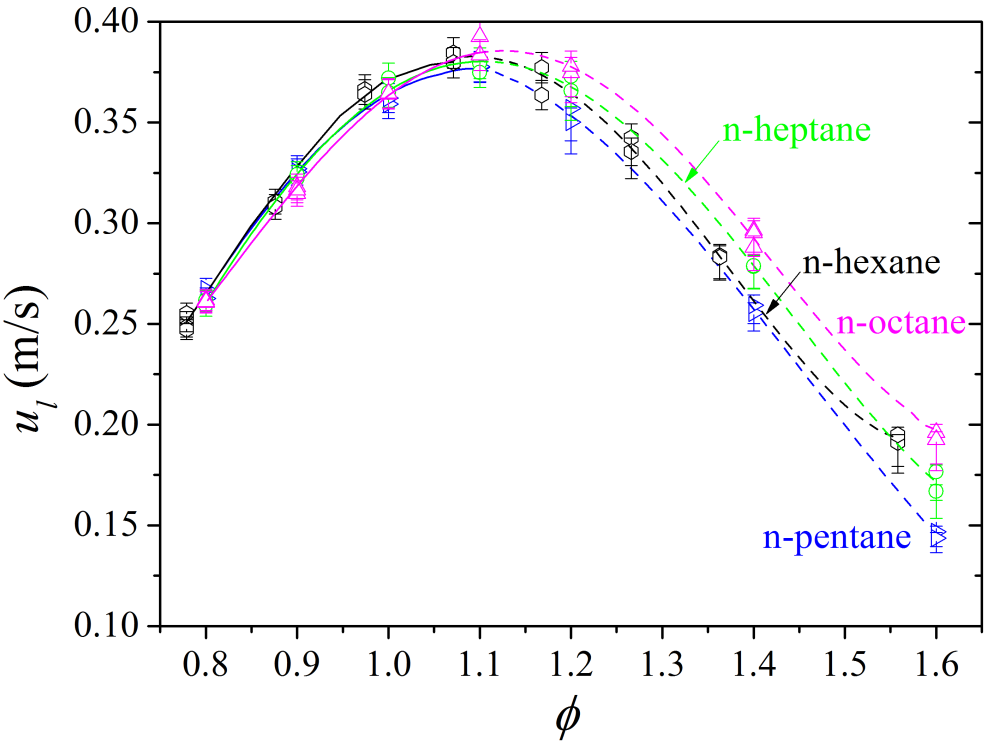

Figure 6 – Laminar burning velocities for n-alkanes, plotted against ϕ. Dashed lines correspond to data computed using $u_l = u_{n,\min}$.

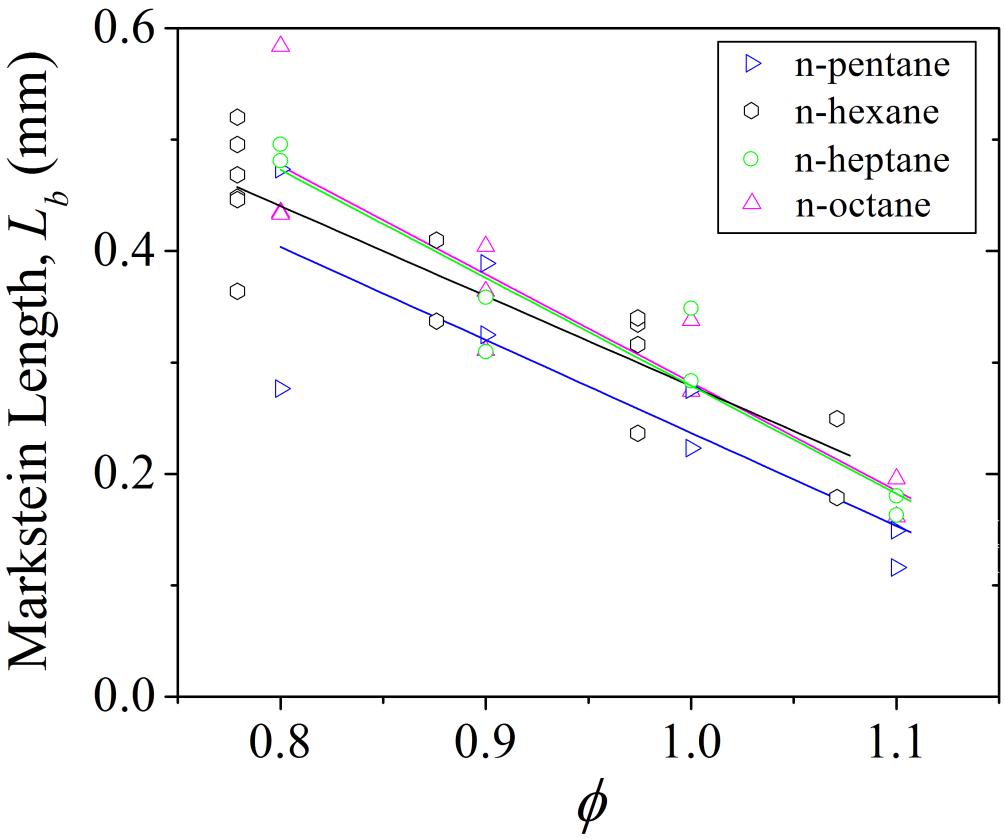

Figure 7 – Measured burnt Markstein lengths of the n-alkanes, plotted against ϕ. Values of L_b of $\phi > 1.1$ mixtures could not be experimentally determined as flames became cellular too early following spark discharge.

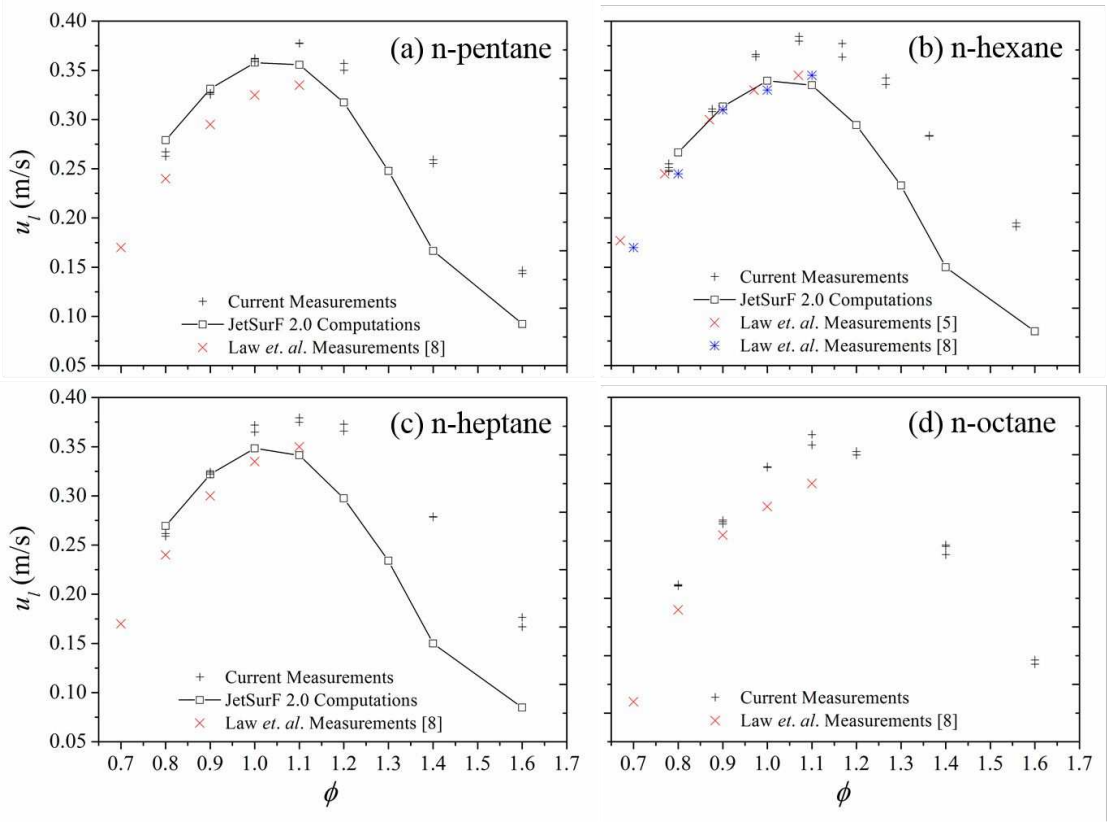

Figure 8 – Comparison between current measurements at 0.5 MPa and 360 K and similar measurements performed in a combustion vessel by Law *et. al*. [5, 8] for n-alkane-air flames at 0.5 MPa and 353 K. Also included for n-pentane through n-heptane (plots (a) through to (c)) are computations performed using the Jetsurf 2.0 mechanism at the same initial temperature and pressure as for the experiments.

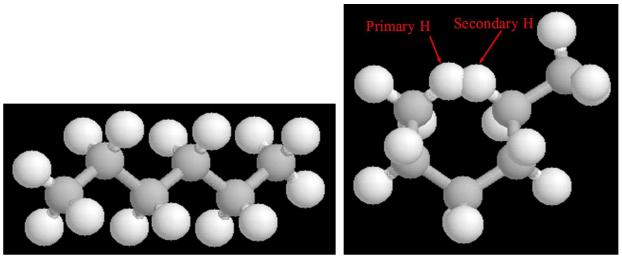

Figure 9 – Molecule of n-hexane (left) and conformation leading to intra-molecular collision between H atoms (right).

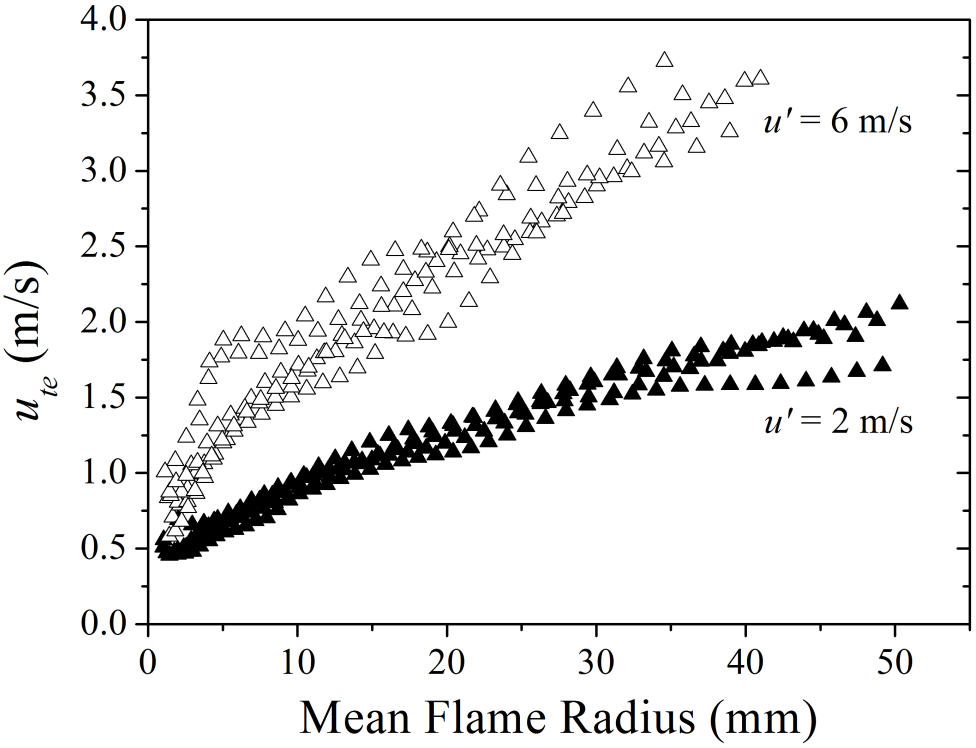

Figure 10 – Development of turbulent n-octane-air flames at *u'* = 2 m/s and 6 m/s, for ϕ = 1.1.

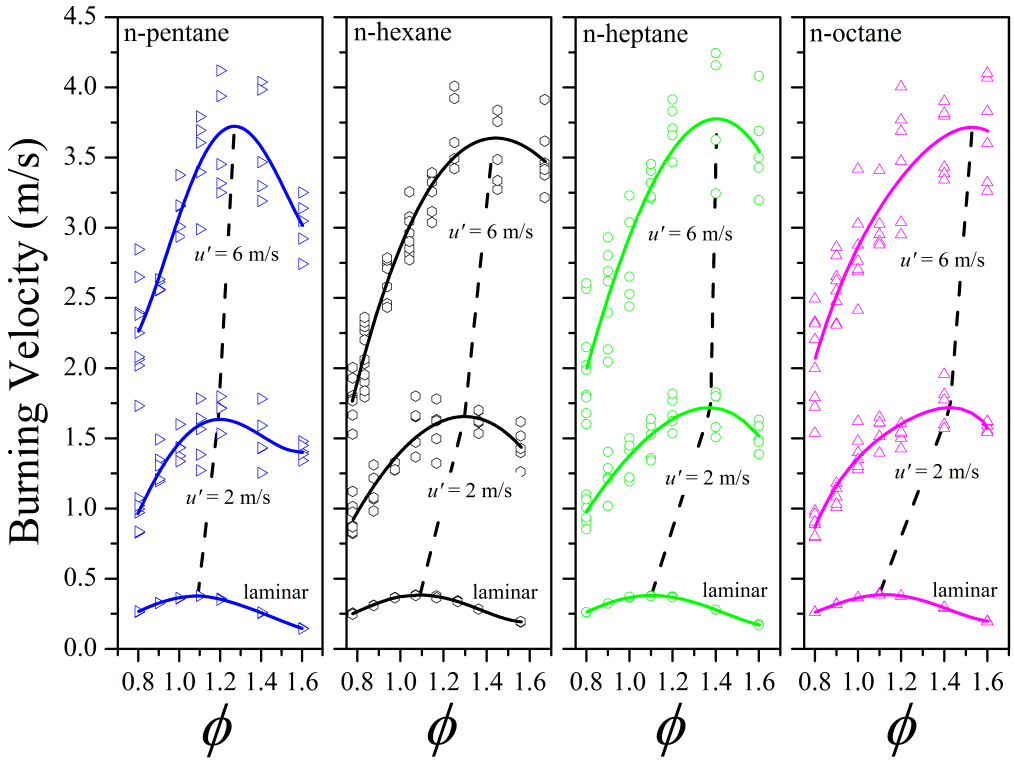

Figure 11 – Laminar and turbulent burning velocities for alkanes of n-pentane through to n-octane. The data fits are third order polynomials, included for illustrational purposes. The dashed lines connect the maximum at each condition.

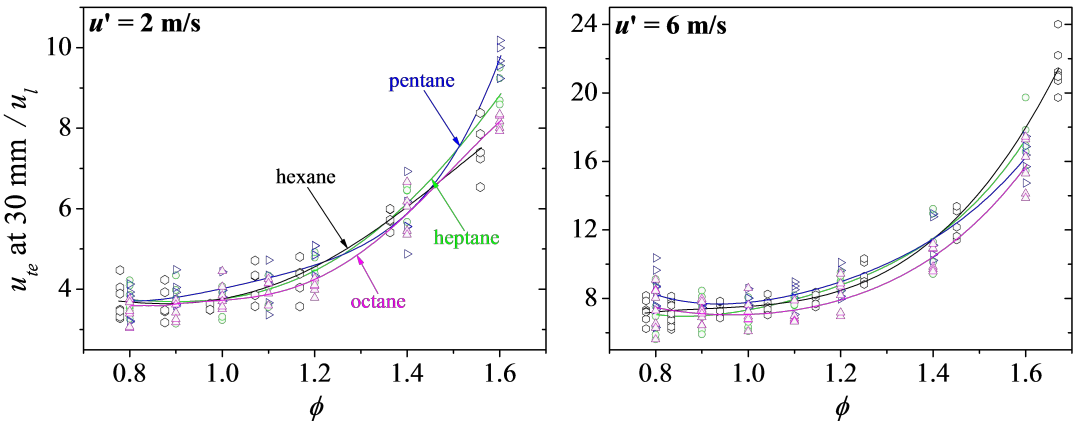

Figure 12 – Ratio of turbulent over laminar burning velocities plotted against ϕ, quantifying the burn rate gains due to turbulence for the n-alkanes investigated.

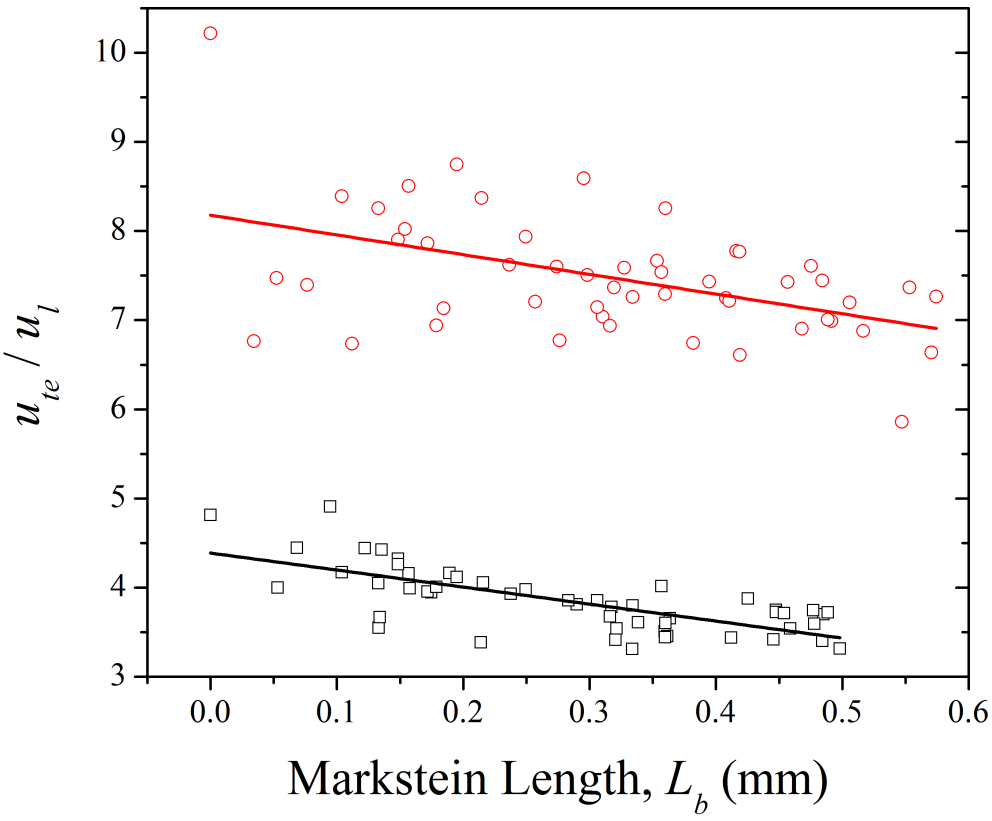

Figure 13 – Overall correlation of u_{te} / u_l with L_b for propane [16], alkanes of C_5-C_8 (current work) and C_6 hydrocarbons of different structure [10] for equivalence ratios of $0.8 \leq \phi < 1.2$ and turbulent r.m.s. velocities of 2 m/s and 6m/s.